Simultaneous Correction for Tracer Arrival Delay and Dispersion in CBF Measurements by the $H_2{}^{15}O$ Autoradiographic Method and Dynamic PET

Ernst Meyer

McConnell Brain Imaging Centre, Montreal Neurological Institute and Department of Neurology and Neurosurgery, McGill University, Montreal, Quebec, Canada

The difference in tracer arrival times between the radial artery and the brain following i.v. injection of ^{15}O-labeled water plus the difference in dispersion of the tracer bolus between these two sites have to be accounted for in order to quantify cerebral blood flow by the autoradiographic approach and positron emission tomography (PET). We describe a method that simultaneously corrects for these two effects by means of a four-parameter fit to the dynamically acquired data. Unlike with other methods, where the two corrections are performed sequentially, no additional measurement of the dispersion time constant is required. We have validated and tested the method by means of simulations and application to data from six human studies. The mean dispersion time constant of 4.0 ± 1.2 sec, estimated by the new method for the six studies, is in fair agreement with estimates of 3 to 5 sec derived from cardiac PET.

J Nucl Med 30:1069–1078, 1989

The i.v. oxygen-15- (^{15}O) labeled water ($H_2{}^{15}O$) bolus method is a widely used technique for the measurement of cerebral blood flow (CBF) with positron emission tomography (PET) (*1–3*). In addition to the quantification of the radioactivity distribution in the brain, this method requires the measurement of the arterial ^{15}O input function that is commonly achieved by rapid manual or automatic blood sampling from the radial artery. This peripheral sampling scheme requires appropriate corrections for: (a) the systematic time difference between the tracer arrival times in the brain relative to the peripheral sampling site (delay correction) and (b) the difference in the degree of distortion in the curve shape of the input function resulting from the dispersion of the tracer bolus in the blood vessels between the heart and the brain on the one hand and between the heart and the radial artery on the other hand (dispersion correction). The critical dependence of calculated CBF values on these two corrections has been previously demonstrated (*2,4,5–8*).

Received Aug. 9, 1988; revision accepted Jan. 24, 1989.

For reprints contact: E. Meyer, PhD, McConnell Brain Imaging Centre, Montreal Neurological Institute, 3801 University St., Montreal, Quebec, Canada H3A 2B4.

A commonly used delay correction method (*7,9*) determines tracer arrival times by linear backward extrapolation of the upslopes of the arterial and whole brain slice radioactivity curves. The input function is then shifted along the time axis by the determined arrival time difference. This empirical method, hereafter referred to as the slope method, has never been validated. Recently, Iida et al. (*1*) have published a more rigorous method for delay correction, hereafter called the global fitting approach, that requires further validation. The same authors (*5*) have described a simple single exponential model to account for dispersion of the arterial input function.

Although the two phenomena, tracer arrival time delay and dispersion, are intimately related, they have been treated in the past as separate entities and the respective corrections were always applied in two consecutive steps. For example, the delay correction may be performed first, followed by the dispersion correction (*5,7*). Reversing the order of correction yields different CBF values when the slope method is used. Ideally, the two corrections should be applied simultaneously.

The present communication describes a method for simultaneous correction for tracer arrival delay and dispersion by means of dynamic curve fitting. Prior to

introducing the new method, various assumptions of the global fitting approach according to Iida et al. (*1*), that are fundamental to the new approach presented here, are assessed, including validation for a two-compartmental system. Also, the limitations of the slope method are demonstrated and the relationship between time delay and dispersion correction examined using simulation and human PET CBF data.

METHODS

PET Procedures

This study was conducted on six young normal volunteers using Positome IIIp (*10*), a two-ring bismuth-germanate (BGO) head machine with transverse and axial spatial resolutions of 11 mm and 16 mm full width at half maximum (FWHM), respectively. A continuous wobbling motion allowed dynamic scanning at a rate of 1 frame per 3 sec and peak total coincidence count rates of 30,000 cps/slice. The true count-rate efficiency of the tomograph is 75 (kC/sec)/(μCi/cc) for the direct slices and 61 (kC/sec)/(μCi/cc) for the cross slice. Reconstruction software includes corrections for detector efficiency variations, random events, and deadtime as well as a deconvolution procedure to eliminate scattered events (*11*). Attenuation correction was performed using a projection thresholding method similar to that of Bergström et al. (*12*). The subjects were positioned in the tomograph with the three image planes centered at 35, 53, and 71 mm above the inferior orbito-meatal line and their heads immobilized by means of a customized selfinflating foam headrest. A short indwelling catheter was placed into the radial artery of one arm for blood sampling and blood gas determinations. For the measurement of CBF, ~ 20 mCi of $H_2{}^{15}O$ were injected as a bolus into the brachial vein of the other arm. Arterial blood sampling and dynamic imaging were started at injection time. A series of 30 sequential PET scans of 3 sec duration each were obtained over 90 sec. The total number of coincidence counts per second of the upper detector ring was recorded at 0.5-sec intervals. Blood samples were collected manually at 3- to 5-sec intervals during the entire data collection period. The sampling catheter was allowed to flow freely at 10 to 15 ml/min causing negligible external dispersion (*5*). Upon completion of the study, the blood samples were assayed in a calibrated well counter in reverse order of their withdrawal for optimal counting statistics. All data were corrected for radioactive decay with respect to injection time based on principles outlined by Raichle et al. (*3*). The first 13 nonzero frames were integrated into a single 39-sec image for each slice. Time delay and dispersion corrections were carried out using various methods described below, and CBF maps were calculated according to Herscovitch et al. (*2*) and Raichle et al. (*3*).

In the following, the theories and methods relevant to the objectives of this communication are summarized.

Delay Correction: Slope Method Versus Global Fitting Approach

We first verified the assumption (*5*) that the total number of coincidence counts per second recorded by a PET detector ring was a good estimate of the total slice tissue activity by comparing the total coincidence counts per second of the upper detector ring, sampled at 0.5-sec intervals, with the total slice time-activity curve obtained from the dynamically reconstructed PET data using 3-sec frames. Next, the time delay corrections, Δt, obtained by various implementations of the slope method and the global fitting approach were examined for a two-compartmental system by simulations. For that purpose, a realistic input function (Fig. 1B) was constructed from a linear combination of gamma functions (*13*) as: $C_a(t) = \sum_{i=1}^{4} a_i t^{n_i} e^{-t/b_i}$ with $a_i = (0.055, 10.0, 0.7, 0.2)$; $n_i = (6.0, 1.0, 1.0, 1.0)$ and $b_i = (1.8, 22.0, 180.0, 300.0)$ for i = 1 to i = 4. With this formulation, contrary to the often used form with $i = n_i = 1$ (*2,4,5*), an inflexion point which is invariably observed on real input functions is produced on the upslope. Ten noiseless tissue time-activity curves, $\bar{C}_t(tm_n)$, representative of a brain tissue element consisting of two compartments with blood flows CBF_1 and CBF_2 and equilibrium tissue-blood partition coefficients for water of $p_1 = 0.82$ and $p_2 = 0.98$ ml/g, were then generated for various combinations of CBF_1 and CBF_2 according to the model equation:

$$\bar{C}_t(tm_n) = \sum_{i=1}^{2} w_i \int_{t_n}^{t_n+\Delta} C_t(t)\, dt = \sum_{i=1}^{2} w_i \int_{t_n}^{t_n+\Delta} C_a(t) * p_i k_i e^{-k_i t}\, dt. \quad (1)$$

Here, w_1 and w_2 are the weighting factors for the two compartments ($w_1 + w_2 = 1$) and the times tm_n represent the midpoints of adjacent data accumulation intervals t_n to $t_n + \Delta$ with $\Delta = 3$ sec. $C_t(t)$ is the instantaneous tissue activity for compartment i, the asterisk stands for the convolution operation and $k_i = CBF_i/p_i$. A first-pass extraction fraction for water of 100% was assumed. For a single tissue compartment and a single data accumulation interval t_1 to t_2 (typically 40 sec), the above equation reduces to the form routinely used for CBF calculation:

$$\int_{t_1}^{t_2} C_i(t)\, dt = \int_{t_1}^{t_2} C_a(t) * p_i k_i e^{-k_i t}\, dt, \quad (2)$$

where the left hand side represents the total counts accumulated from time t_1 to t_2 for tissue element i.

The tracer arrival time difference, Δt, between $C_a(t)$ and $\bar{C}_t(tm_n)$ was first determined by the slope method (Fig. 1B) and compared to the theoretically correct value assumed to be $\Delta t_{th} = 0$ sec for this simulation. The tracer arrival times at the brain tissue level and in the peripheral arterial blood were determined by linear backward extrapolation of the upslopes of the arterial blood and the whole brain slice curves. In the case of manual blood sampling, the slope is usually determined by drawing the tangent to the rising portion of the curve by visual approximation (Fig. 1B) since this discontinuous sampling scheme does not allow an accurate determination of the time at which $C_a(t)$ becomes larger than zero. For continuously sampled curves, linear least-squares fitting between 20% and 50% of the curve peak height has been suggested (*7*).

The same simulation data were then used to determine Δt by the global fitting approach as implemented by Iida et al. (*1*). With this approach, the whole slice time-activity curve, $X(t)$ (e.g., represented by the detector ring total coincidence counts per second), is approximated by a convolution integral

of the form:

$$X(t) = C_a(t + \Delta t) * Ae^{-Bt}, \quad (3)$$

where Δt is the global time delay between the measured arterial and the whole brain slice curves, and A and B are arbitrary parameters. Equation (3) is a single integral adaptation of Eq. (2) for the case of a one-compartmental system ($i = 1$). $C_i(t)$ the brain tissue level and in the peripheral arterial blood were tation of Iida et al. (*1*), A and B were first fitted for various fixed delays, Δt. The parameter triplet for which the error criterion was minimized was then chosen. The double integral formulation was not deemed necessary given the usually short (0.5 to 3 sec) sampling interval for $X(t)$.

In our implementation, the three parameters, A, B, and Δt, were fitted simultaneously. This was achieved by substituting u for $t + \Delta t$ which transformed Eq. (3) into:

$$X(t) = Ae^{-B(t+\Delta t)} \int_{\Delta t}^{t+\Delta t} C_a(u)e^{Bu}\, du \quad (4)$$

a form that is easily amenable to nonlinear least squares fitting. Notice that $C_a(t)$ is the arterial input function measured at the peripheral sampling site. The fitted value for Δt was again compared to the correct value of $\Delta t_{th} = 0$ sec. The nonlinear least squares fitting procedure used here was based on the algorithm of Marquardt as implemented by Bevington (*14*).

Delay Versus Dispersion Correction: Effect on Calculated CBF

The time delay correction is required in order to determine the common zero time for the arterial and brain tissue curves. If the measured input function is shifted along the time axis by the arrival time difference, Δt, then the model Eq. (1) has a common time scale and satisfies the initial conditions $C_i(0) = 0$ and $C_a(0) = 0$.

Dispersion correction of the input function in various models has been treated by several authors (*5,8,15,16*). Iida et al. (*5*) used a simple monoexponential dispersion function of the form:

$$d(t) = \frac{1}{\tau} exp\left(\frac{-t}{\tau}\right), \quad (5)$$

where τ is the dispersion time constant. The peripherally measured dispersed input function, $g(t)$, and the true, dispersion corrected, input function, $C_a(t)$, are related to each other as follows:

$$g(t) = C_a(t) * d(t) \quad (6)$$

with the asterisk again standing for the convolution operation.

Using Laplace transforms to deconvolve Eq. (6) (*5,7*), Eq. (2) can be expressed in terms of the observed dispersed input function, $g(t)$, as:

$$\int_{t_1}^{t_2} C_i(t)\, dt = \int_{t_1}^{t_2} [\tau pkg(t) + (1 - \tau k)g(t) * pke^{-kt}]dt. \quad (7)$$

Using our human data, we first calculated CBF according to equation (7), which implicitly accounts for dispersion, after having performed the delay correction by the slope method using $g(t)$. An integration interval of $t_2 - t_1 = 39$ sec was used.

As a second step, we first calculated the dispersion corrected input function, $C_a(t)$, by deconvolution according to Eq. (6), assuming an estimated dispersion time constant of $\tau = 5$ sec (*5*). Using Laplace transforms, it can be shown that $C_a(t)$ may be calculated as:

$$C_a(t) = g(t) + \tau \frac{dg}{dt}. \quad (8)$$

The delay correction was then performed by the slope method using $C_a(t)$ and CBF calculated according to Eq. (2). This formulation is mathematically equivalent to Eq. (7) where $C_a(t)$ simply had been substituted by $g(t)$ according to Eq. (6) (*5*), the only difference being the time delay used here, which was different from that found in the previous step. Again, an integration interval of $t_2 - t_1 = 39$ sec was used and the CBF values calculated in the two steps compared for selected regions of interest (ROIs).

Simultaneous Correction for Delay and Dispersion

In an effort to achieve simultaneous correction for both time delay and dispersion, the global fitting approach was extended to include the dispersion time constant, τ, as a fourth fitting parameter. This was achieved by reformulating Eq. (7) in its single integral form and adapting it to the whole slice version in the sense of Eq. (3), using the same substitutions as before:

$$X(t) = \tau Ag(t + \Delta t) + (1 - \tau B)g(t + \Delta t) * Ae^{-Bt}. \quad (9)$$

Equation (9) was rearranged into a form suitable for nonlinear least-squares fitting by substituting u for $t + \Delta t$ and explicitly expanding the convolution operation:

$$X(t) = \tau Ag(t + \Delta t) + (1 - \tau B)Ae^{-B(t+\Delta t)} \int_{\Delta t}^{t+\Delta t} g(u)e^{Bu}\, du. \quad (10)$$

The value of $g(t + \Delta t)$ was obtained by cubic spline interpolation of the discretely measured peripheral input function.

In order to assess the feasibility of the simultaneous correction approach, ten tissue time-activity curves were generated for a two-compartmental system as described above using Eq. (1) with mean CBF values ranging from 10 to 75 ml/min/100 g. The input function, $C_a(t)$, was then shifted along the time axis by Δt sec and dispersed according to Eq. (6) using a dispersion time constant of $\tau = 5$ sec in order to generate $g(t)$, the input function observed in a real situation. The four-parameter fit performed according to Eq. (10) on $g(t)$ and the simulated noiseless tissue curves yielded estimates of Δt and τ that were then used to calculate mean CBF by the polynomial interpolation approximation according to Raichle et al. (*3*), the method currently used for CBF calculation in our human studies. This first simulation allowed us to assess the accuracy with which Δt, τ, and CBF could be recovered in an ideal situation. Next, ten random noise patterns were superposed onto each of the ten tissue curves (*9,17*) and Δt, τ, and CBF again determined as just described. This second simulation served to evaluate the accuracy and precision (mean ± s.d.) of the fitted estimates for Δt and τ in a real situation and to study the effect of propagation of uncertainties in these two parameters into the final calculation of CBF. The newly proposed simultaneous correction method was then applied to our human data with $X(t)$ represented by the total coincidence counts per second of the upper detector ring and the

results compared with CBF determinations from other methods.

RESULTS

Figure 1A shows the tissue curve of the entire upper slice, reconstructed with a 3-sec frame interval, superposed onto the curve representing the total number of coincidence counts per second for the upper detector ring. The latter curve was sampled at 0.5-sec intervals and corrected for radioactive decay only. The two curves virtually coincide during the first 40 to 60 sec after tracer injection and may therefore be used interchangeably for the purpose of time delay corrections. This was further confirmed by the fact that the time delay, Δt_{fit}, determined by the fitting approach for the six human studies differed by an average of only 0.4 sec or less using the two types of curves (Table 1).

Figure 1B illustrates the limitations of the slope method. A simulated input function, sampled at 5-sec intervals, is shown together with the corresponding tissue curve. The manually drawn tangents to the upslopes of the two curves are indicated with their zero

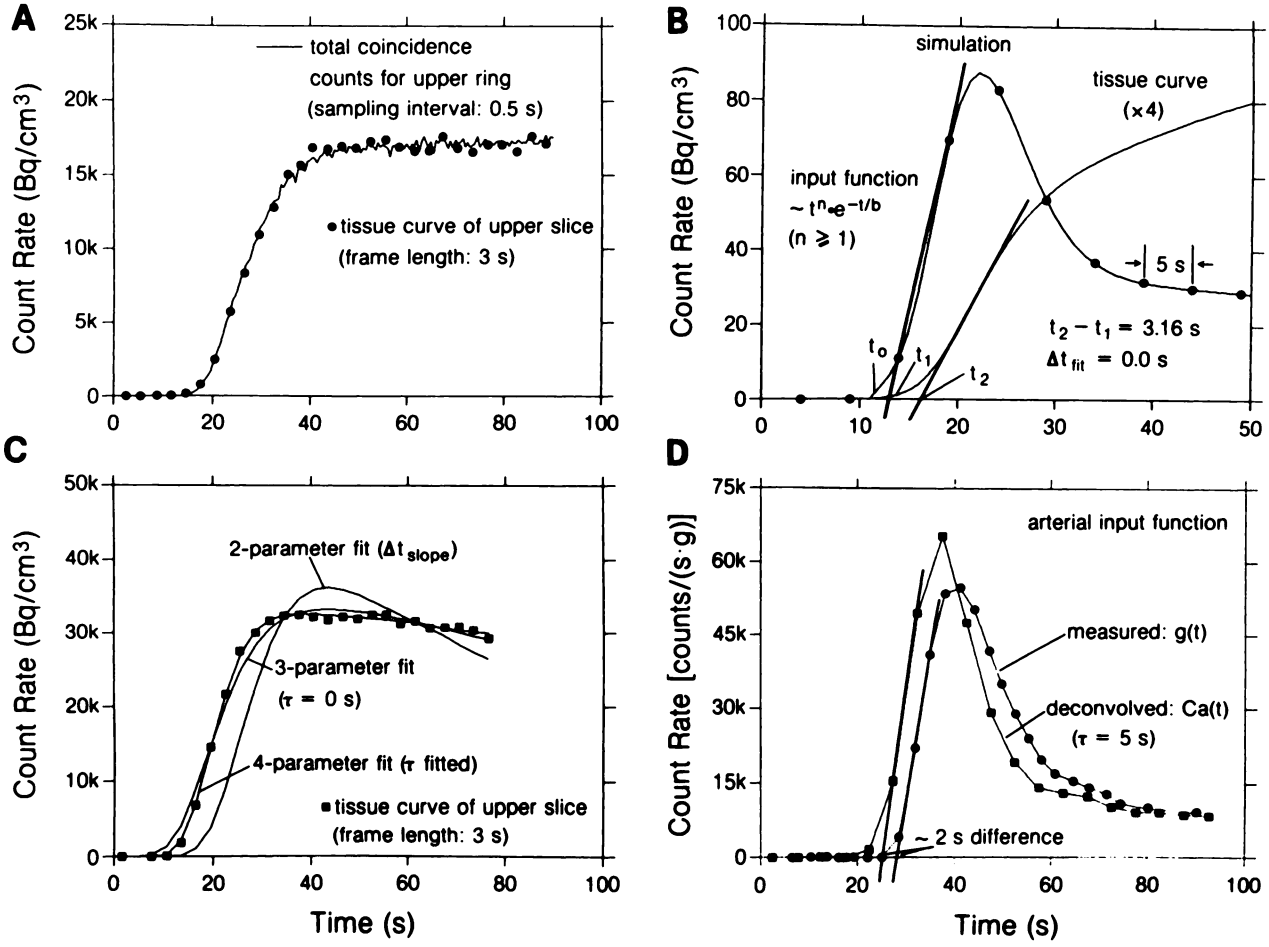

FIGURE 1

A: Total, decay corrected, coincidence count rate of upper detector ring sampled at 0.5-sec intervals (continuous line) superposed onto upper slice tissue curve (solid black circles) reconstructed with a frame length of 3 sec. B: Illustration of slope method for determination of tracer arrival time differences, Δt, between peripheral arterial blood and brain. Shown are a simulated input function (5-sec blood sampling interval, solid black circles) and the corresponding tissue curve for a brain volume element consisting of two equally weighted compartments with blood flows $CBF_1 = 20$ and $CBF_2 = 80$ ml/min/100g and equilibrium tissue-blood partition coefficients for water of $p_1 = 0.82$ and $p_2 = 0.98$ ml/g. The time intercepts of the visually drawn slopes give a wrong Δt of $t_2 - t_1 = 3.16$ sec as compared to the theoretically correct value of $\Delta t_{th} = 0$ sec. C: Tissue time-activity curve of upper slice (solid black squares) together with three fitted tissue curves (see Eq. 10 in text). For the two-parameter fit, a fixed time delay determined by the slope method, Δt_{slope}, was used. For the three-parameter fit, the time delay, Δt, was fitted as a third parameter. In the four-parameter fit, the dispersion correction time constant, τ, was included as a fourth fitting parameter. The significantly better three- and four-parameter fits are apparent. D: Illustration of slope method (visual approximation) applied to measured ($g(t)$) and deconvolved, i.e., dispersion corrected ($Ca(t)$), input functions using a dispersion correction time constant of $\tau = 5$ sec. The time intercepts of the two slopes differ by ~ 2 sec.

TABLE 1
Time Delays, Δt_{fit}, Determined by Fitting Approach*

Case ID	Δt_{fit} [s] (τ = 0 sec) u.s.c.c.	u.s.	(τ = 5 sec) u.s.c.c.	u.s.
1	5.3	6.5	2.4	3.7
2	5.5	5.0	2.8	2.4
3	8.9	10.0	6.8	8.0
4	9.4	10.1	7.2	7.7
5	13.3	13.1	10.4	10.3
6	13.7	13.4	11.0	10.8
Difference (s.d.)	0.3 (0.7) sec (N.S.)		0.4 (0.7) sec (N.S.)	

paired Student's t-test

* Between the arterial input function and the upper slice total coincidence counts (u.s.c.c.) on the one hand and between the input function and the reconstructed tissue curve of the upper slice (u.s.) on the other hand as determined by a 40-sec three-parameter fit with dispersion correction time constants of τ = 0 s and r = 5 sec, respectively. Data obtained on six young healthy volunteers.

TABLE 2
Simulation Study with Noiseless Data‡

CBF_1	CBF_2 [ml/min/100 g]	$\overline{CBF}$*	$\Delta t_{slope\ (vis)}$ [sec]	$\Delta t_{slope\ (back)}$ [sec]	Δt_i† [sec]	Δt_{fit} [sec]
10	10	10	3.25	−6.20	−1.03	−0.04
10	20	15	3.12	−3.54	−0.90	−0.02
10	30	20	3.35	−2.06	−0.73	−0.04
20	30	25	3.39	−2.11	−0.71	−0.01
20	40	30	3.39	−0.31	−0.60	0.01
20	50	35	3.44	0.54	−0.53	0.01
20	60	40	3.62	0.90	−0.51	0.01
20	80	50	3.16	2.14	−0.46	0.03
20	100	60	3.21	2.29	−0.42	0.04
30	120	75	3.21	2.46	−0.38	0.05
Mean (n = 10)			3.31	−0.59	−0.63	0.0040
(s.d.)			(0.15)	(2.85)	(0.21)	(0.0313)

* The mean blood flow was calculated as $\overline{CBF} = w_1CBF_1 + w_2CBF_2$ assuming weighting factors of $w_1 = w_2 = 0.5$.

The backward extrapolation was done on the upslope of the blood and tissue curves between 20% and 50% of the peak height. A 60-sec fit interval was used for Δt_i and Δt_{fit}.

† Here, the fit was carried out for three delays, namely −5 sec, 0 sec, and + 5 sec, and the "best" delay determined by parabolic interpolation.

‡ Time delays, Δt, between the tracer arrival time in peripheral arterial blood and the brain determined by the slope method (vis: visual approximation, back: backward extrapolation) and the fitting approach as implemented by Iida et al. (*1*) (Δt_i)† or as proposed in the present study (Δt_{fit}). A single blood curve (linear combination of gamma functions, see Fig. 1b and Methods) was used to generate ten tissue curves (see equation (1) in text) for a brain tissue element consisting of two compartments with blood flows CBF_1 and CBF_2 and water tissue-blood partition coefficients of p_1 = 0.82 and p_2 = 0.98 ml/g. The theoretically correct delay was Δt_{th} = 0 sec.

intercepts t_1 and t_2 from which a time delay (Δt_{slope}) of $t_2 - t_1$ = 3.16 sec was calculated. In fact, the two simulated curves had a common theoretical zero time intercept of t_{th} = 0 sec that was accurately recovered with the fitting approach (Δt_{fit} = 0 sec). The results of a simulation study with noiseless data, comparing the time delays obtained by the slope method and the fitting approach are summarized in Table 2 for ten selected combinations of CBF_1 and CBF_2 of a two-compartmental system. The second last column (Δt_I) shows the result of an implementation of the global fitting method according to Iida et al. (*1*) where the fit was carried out for three selected time delays, namely −5 s, 0 sec, and +5 sec, and the "best" delay determined by parabolic interpolation. Although these results are within 1 sec of the true value, the better accuracy achieved by simultaneously fitting A, B, and Δt as proposed in this paper (Eq. 4) is evident from the results in the last column. Selection of a larger number of time delays spaced very closely (e.g., every 0.1 sec), of course, would improve the results obtained by the interpolation approach, however, on the expense of increased computing time. The slope method was consistently wrong by ~ 3.3 sec with the visual approximation and by −6.2 to 2.5 sec with the backward extrapolation. The superiority of the fitting approach over the slope method is further illustrated in Figure 1C where a measured whole slice time-activity curve is shown together with three curves, all fitted according to Eq. (10). For the first curve (two-parameter fit for A and B), a fixed Δt, determined by the slope method, was used. For the second curve (three-parameter fit), the time delay, Δt, was fitted as a third parameter. When the dispersion time constant, τ, was included as a fourth fitting parameter, a quasi perfect fit was obtained (four-parameter fit). The significantly better three- and four-parameter fits are visually apparent and substantiated by the smaller chi-square (goodness of fit) values of 2.47 and 0.26, respectively, compared to 42.8 for the two-parameter fit.

The results of the stimulation study regarding the simultaneous correction for time shift and dispersion of the input function (four-parameter fit) are shown in Table 3,A and B for two theoretical values of Δt and τ_{th} = 5 sec. The noiseless data indicate that there is some interaction between the fitted values of Δt and τ in that the two parameter estimates deviate by 2% to 10% from their true values in opposite directions, i.e., when τ_{fit} was below its true value, then Δt_{fit} was always slightly high, and vice versa. These opposing inaccuracies in Δt and τ virtually cancelled each other in the calculation of CBF as illustrated by the negligible difference between CBF_{th} and CBF_{calc} for the noiseless data. The results for the noisy data were very similar with average

TABLE 3

A: Simulation Study with Simultaneous Correction for Time Shift and Dispersion of the Input Function:

	Noiseless data			Noisy data (5%)		
CBF_{th} [ml/min/100 g]	Δt_{fit} [sec]	τ_{fit} [sec]	CBF_{calc} [ml/min/100 g]	Δt_{fit} [sec]	τ_{fit} [sec]	CBF_{calc} [ml/min/100 g]
10	0.42	4.79	10.0	0.29 (0.21)	4.43 (0.96)	10.1 (0.2)
15	0.42	4.83	14.9	0.42 (0.25)	4.91 (1.58)	14.9 (0.7)
20	0.41	4.84	19.9	0.40 (0.24)	4.84 (1.49)	19.8 (0.9)
25	0.39	4.74	24.9	0.42 (0.23)	4.86 (1.48)	24.8 (1.2)
30	0.38	4.76	29.9	0.52 (0.48)	4.71 (1.23)	29.8 (1.4)
35	0.40	4.80	34.8	0.41 (0.23)	4.85 (1.48)	34.7 (1.8)
40	0.38	4.75	39.9	0.35 (0.22)	4.43 (1.16)	40.2 (1.4)
50	0.39	4.77	49.8	0.35 (0.22)	4.42 (1.15)	50.2 (1.8)
60	0.39	4.79	59.8	0.43 (0.38)	4.74 (1.40)	59.6 (3.2)
75	0.39	4.80	74.8	0.29 (0.19)	4.82 (1.30)	75.3 (3.8)
mean (n = 10)	0.40	4.79		0.39	4.70	
(s.d.), (s.e.m.)*	(0.02)	(0.03)		(0.07)*	(0.20)*	
B: Simulation Study: Conditions as for A, Except for Δt_{th} = 5 SEC.						
10	4.44	5.11	10.1	4.28 (0.67)	5.51 (1.42)	10.0 (0.2)
15	4.44	5.15	15.1	4.52 (0.60)	5.32 (2.01)	15.1 (0.6)
20	4.46	5.14	20.2	4.66 (0.56)	4.95 (1.69)	20.2 (0.8)
25	4.49	5.00	25.3	4.48 (0.64)	5.29 (1.93)	25.2 (1.2)
30	4.50	5.04	30.4	4.52 (0.60)	5.32 (1.99)	30.1 (1.5)
35	4.47	5.11	35.4	4.65 (0.55)	5.05 (1.70)	35.3 (1.6)
40	4.50	5.02	40.5	4.51 (0.58)	5.34 (1.95)	40.1 (2.0)
50	4.49	5.06	50.6	4.52 (0.57)	5.33 (1.94)	50.1 (2.6)
60	4.50	5.07	60.6	4.52 (0.57)	5.31 (1.91)	60.1 (3.1)
75	4.49	5.10	75.7	4.51 (0.56)	5.37 (1.92)	75.1 (3.9)
mean (n = 10)	4.48	5.08		4.52	5.28	
(s.d.), (s.e.m.)*	(0.02)	(0.05)		(0.10)*	(0.16)*	

* Time delays, Δt, between the tracer arrival time in peripheral arterial blood and the brain, and dispersion time constants, τ, determined simultaneously by nonlinear least squares fitting on noiseless data and on data with 5% random noise superposed. Tissue curves were generated according to Eq. (1) (see text) for a two-compartmental model with mean blood flow CBF_{th}. A linear combination of gamma functions (see Fig. 1B and Methods) was used to simulate the arterial blood curve. Water tissue-blood partition coefficients of $p_1 = 0.82$ and $p_2 = 0.98$ ml/g were used. The theoretically correct values for τ and Δt were: $\tau_{th} = 5$ s and $\Delta t_{th} = 0$ sec. Calculated blood flow, CBF_{calc}, was obtained by the polynomial approximation method of Raichle et al. (3).

inaccuracies in Δt and τ of half a second or less. Mean calculated blood flows, CBF_{calc}, were within 1% of their true values with coefficients of variation (100% × mean/s.d.) between 2% and 5.5% only. For this simulation, the fitting parameters were constrained to non-negative values in order to guarantee meaningful results and to avoid negative values in the early portion of the fitted tissue curves (undershoot). This constraint was not unrealistic since for the common case of arterial sampling from an arm or leg, Δt and τ are very unlikely to become negative and A and B are positive by definition (see Methods). On a few occasions, extension of the fit interval from 40 to 60 sec was necessary in order to reach convergence within 50 iterations. A 5% noise level was judged appropriate to simulate conditions met in real studies as seen by comparing Figures 1A and C with Figure 2.

The effect on calculated CBF of the sequence in which the delay and dispersion corrections are applied was compared to the case where both corrections are carried out simultaneously as illustrated in Table 4 where mean gray and white matter blood flows are listed for the six human studies calculated for various conditions. In each study, four circular ROIs with a diameter of 2 cm were placed over temporal gray matter and two ROIs with a diameter of 1.2 cm over white matter of the centrum semiovale. For the CBF values in the first column, the delay and dispersion corrections were carried out simultaneously with Δt and τ estimated from the four-parameter fit. The mean of these values was set to 100% (reference values). The second column lists CBF values calculated by the conventional method, i.e., without dispersion correction and with the time delay determined by the slope method using $g(t)$. These

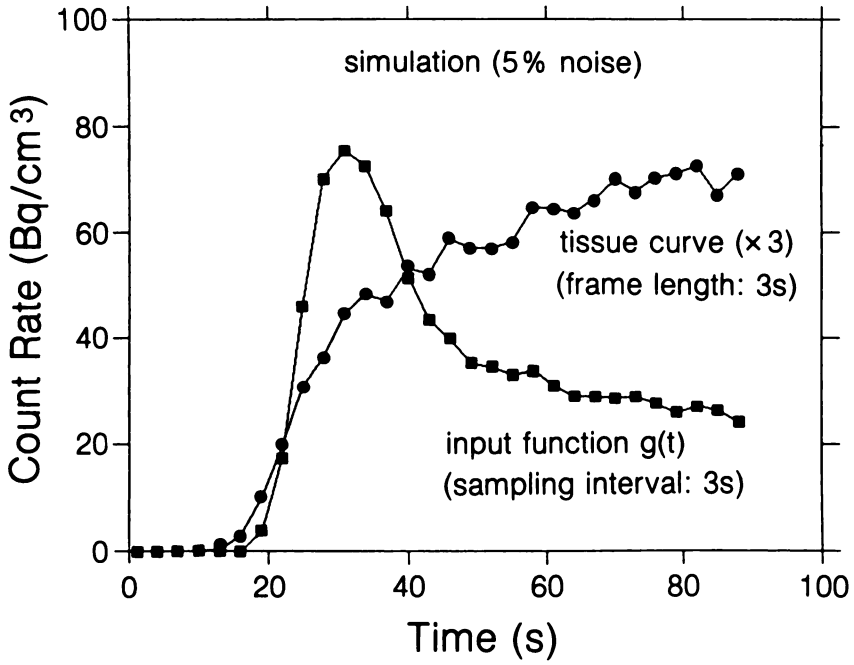

FIGURE 2
Simulated blood (circles) and tissue (squares) data with 5% random noise superposed. The input function was dispersed with a dispersion time constant of $\tau = 5$ sec (see Eqs. (5) and (6) in text) and shifted by $\Delta t = 5$ sec to the right on the time axis. The tissue curve was generated according to Eq. (1) (see text) for a brain volume element consisting of two equally weighted compartments with blood flows $CBF_1 = 20$ and $CBF_2 = 80$ ml/min/100 g and equilibrium tissue-blood partition coefficients for water of $p_1 = 0.82$ and $p_2 = 0.98$ ml/g. The sampling interval for both curves was 3 sec.

values are almost 25% above the reference level. This is explained by the following two facts.

1. As pointed out by Iida et al. (*1*), and confirmed by the present study (Table 5), the time delays determined by the slope method are too short. As an example, a 4-sec underestimation in the time delay may result in an overestimation of as much as 20% in CBF calculated for a data accumulation interval of 40 sec (*5,7*).

2. Neglecting the dispersion correction leads to an overestimation of CBF. For a 40-sec data accumulation interval and a flow value of 40 ml/min/100 g, this overestimation, depending on the shape of the input function, may amount to as much as 15% (*5*). The values in the third column were calculated with the delay correction being performed first, using the slope method and $g(t)$, followed by the dispersion correction with an estimated dispersion time constant of $\tau = 5$ sec (*5,7*). These values are slightly below the reference level. Here, it appears that the overestimation of CBF expected from the incorrect delay correction provided by the slope method was effectively compensated for by

TABLE 4
Effect on the Calculated CBF Value of the Sequence in Which the Time Delay and Dispersion Corrections are Applied as Compared to the Case Where Both Corrections are Carried out Simultaneously‡

	CBF [ml/min/100 g]				
	Simultaneous delay and disp. corrections (fit approach)	Delay corr. by slope method, no dispersion correction	Delay corr. by slope method, followed by disp. corr.	Disp. corr., followed by delay corr. by slope method	Delay corr. by fit method, no dispersion correction
Gray:	63 ± 13 (100%)	78 ± 16 (124%)*	62 ± 14 (98%)	72 ± 15 (114%)*	65 ± 14 (103%)
White:	26 ± 4 (100%)	32 ± 6 (123%)†	25 ± 5 (96%)	30 ± 5 (115%)†	27 ± 4 (104%)

Values are mean ± s.e.m. (n = 24 ROIs for gray and n = 12 ROIs for white matter).
A dispersion time constant of $\tau = 5$ s was used for the results in columns 3 and 4.
* Significantly different from control (100%) at $p < 0.01$ by Newman-Keuls test.
ANOVA: $F_{4,20} = 33.5$; $p < 0.00001$.
† Significantly different from control (100%) at $p < 0.01$ by Newman-Keuls test.
ANOVA: $F_{4,20} = 24.2$; $p < 0.00001$.
CBF calculated for a 39 sec data accumulation interval.
Mean $PaCO_2$ for the six studies: 36.9 ± 3.6 mm Hg.
‡ Results for gray and white matter from six young healthy volunteers.

the dispersion correction performed on the incorrectly shifted input function. The next column shows values where the dispersion correction was carried out prior to the delay correction. The ~ 15% overestimation of CBF by this method is explained by the fact that the upslope of the deconvolved, i.e., dispersion corrected, input function, $C_a(t)$, is shifted by a few seconds to the left on the time axis relative to the measured input function, $g(t)$ (see Fig. 1D). As a consequence, the time delay determined by the slope method and $C_a(t)$ is smaller than that determined with $g(t)$ which, in turn, is already smaller than the delay found with the global fitting approach. Therefore, in agreement with predictions from simulations (*2,4–7*), the calculated CBF for this condition represents an overestimate. In particular, the results in columns 3 and 4 are significantly different from each other. The values in the last column, calculated with the fitted time delay, illustrate the effect of ignoring dispersion. The relatively small overestimation of CBF found here may be due to the particular shape of the input function [a sharply peaked function tends to reduce the effect of ignoring dispersion (*5*)]. Furthermore, the highly nonlinear nature of the error imposed on calculated CBF by inaccuracies in both Δt (*7*) and τ (*5*) has to be kept in mind when interpreting Table 4. The results in columns 2 and 4 were significantly different from the reference values in column 1 at the $p < 0.01$ level as indicated by an analysis of variance (ANOVA) with post-hoc testing according to Newman-Keuls (*18*).

Table 5 lists time delays, Δt, determined in the six human studies for various conditions. The first column gives delays obtained by the slope method and $g(t)$ without dispersion correction. Next, the values determined with the global fitting approach and without dispersion correction are listed. The means of the two columns differ by 3.8 sec, in good agreement with the finding of Iida et al. (*1*). Using the fit method and a dispersion correction with $\tau = 5$ sec gives delays that are, on average, only 1.3 sec longer than those obtained with the slope method and no dispersion correction. Fitting of the dispersion constant τ as a fourth parameter (column 4) did not result in any significant additional change in Δt compared to column 3. The last column gives values of the fitted dispersion time constant. Its mean of $\tau = 4.0$ sec is in fair agreement with the estimate of 3–5 sec derived from cardiac PET studies (*5*).

DISCUSSION

Most current quantitative PET procedures require sampling of the arterial concentration of the radiolabel being used (input function). Ideally, in order to satisfy the model assumptions, the blood sampling should occur at the same level as the PET tissue activity measurement. For cerebral PET studies, this requirement is difficult to meet. The problems arising from peripheral arterial sampling, therefore, are not unique to the intravenous $H_2{}^{15}O$ bolus autoradiographic CBF method where the radial artery is commonly used for that purpose. Truly quantitative CBF estimates com-

TABLE 5
Time Delay Determined by the Slope and the Fit Method†

	Δt [sec]				
Case ID	Slope method, no disp. corr.	Fit method, no disp. corr.	Fit method with disp. corr. (τ = 5 sec)	Fit method with disp. corr. (τ fitted)	τ_{fit} [sec]
1	1.7	5.3	2.4	3.0	3.0
2	2.6	5.5	2.8	2.6	5.6
3	5.4	8.9	6.8	7.3	2.8
4	4.5	9.4	7.2	7.6	3.1
5	9.9	13.3	10.4	10.4	5.0
6	8.9	13.7	11.0	11.0	4.7
mean	5.5	9.3	6.8	7.0	4.0
(s.d.)	(3.3)	(3.6)	(3.6)	(3.6)	(1.2)
difference (s.d.)	3.8 (0.8)		0.2 (0.3)		
	$p < 0.01$)*		(N.S.)*		
	1.3 (1.0)				
	($p < 0.01$)*				

* Paired t-test with Bonferroni's correction for multiple comparisons.

† Δt, between arterial input function and tissue curve (upper slice coincidence counts) determined by the slope and the fit method (40 sec fit interval), respectively, with and without dispersion correction on six young healthy volunteers. The values of the fitted dispersion time constant, τ, are also shown.

parable to values obtained with other techniques (*19*), however, may be obtained by this method if the transit time difference between the left ventricle of the heart and the brain on the one hand and the left ventricle and the peripheral sampling site on the other hand (delay correction) as well as the ensuing difference in the shape of the tracer bolus (dispersion correction) are properly accounted for. Since the difference in bolus distortion is a direct consequence of the transit time difference between the brain and the sampling artery, we are proposing a correction method that simultaneously accounts for these two phenomena. Prior to implementing this new method, various aspects relating to the underlying model (*1*) required further validation and results obtained with other methods were also analyzed.

The simultaneous correction method presented in this paper unites two methods that have been recently developed to separately correct for time delay (*1*) and dispersion (*5*). By adding the dispersion time constant, τ, as a fourth parameter to the model previously introduced by Iida et al. (*1*) for delay correction alone, we obtained fairly accurate simultaneous estimates of time delay, Δt, and dispersion time constant, τ, as verified by simulations. The extended model also gave a better fit to the dynamic tissue data (Fig. 1C). With regard to its practical application to the calculation of CBF, we found that errors in the estimates for Δt and τ by the new method always had opposite signs and, therefore, only minimally affected the calculated CBF values. The simultaneous correction method makes a separate measurement of the dispersion time constant, e.g., by cardiac PET imaging (*5*), unnecessary and avoids the use of an average value for τ. It also eliminates the ambiguities in calculated CBF caused by the various possible ways to treat the two corrections sequentially (Table 4).

Our validation of the suggestion by Iida et al. (*1*) that the total coincidence count curve of a PET detector ring could be substituted for the whole slice tissue curve and used for delay correction (Table 1) is of practical importance since this curve is easily acquired on line and requires less computer processing and storage than the dynamic reconstruction of the whole slice tissue curve.

We present simulations (Fig. 1B, Table 2) that indicate that time delays determined by the slope method, an empirical procedure that had never been validated, may be wrong by several seconds resulting in a 10% to 20% error in CBF for a 40-sec data accumulation time (*2,5,7*). This is not surprising since the tissue curve, after the first few seconds of acquisition, is corrupted by the washout of tracer from the tissue which is blood flow dependent. The linear combination of gamma functions that we used for a more realistic simulation of the arterial input function (*2,5*) was crucial to the assessment of the slope method. Our simulations, on the other hand, lend support to the global fitting approach of Iida et al. (*1*) which we have validated for a two-compartmental system (Table 2). The possible tracer arrival time difference between the two compartments (*1*), however, was not taken into account in this simulation. The fitting algorithm described by Iida et al. (*1*) was improved, both from a theoretical as well as from a practical point of view, to allow truly simultaneous fitting of all parameters (Eq. 4). This was achieved by a translation of the time scale that shifted the time delay parameter from the argument of the input function to the integration limits (*20,21*).

From our six human studies we found that the time delays determined by the slope method systematically underestimated the fitted delays by an average of 3.8 sec when dispersion effects were neglected, leading to an overestimation of CBF by ~ 20% for a data accumulation interval of 40 sec. This is in agreement with data from Iida et al. (*1*) and not only confirms the reproducibility of the fit method but also demonstrates that it may be equally well applied to continuously (*1*) as well as manually (this study) sampled blood data.

When a dispersion correction was included in the fitting approach, the difference between the time delay by the new method and that from the conventional slope method, without dispersion correction, was reduced to ~ 1.5 sec. This small timing difference resulting from the two methods should not detract from the fact that the CBF values calculated with the dispersion corrected input function, in general, are substantially smaller than those calculated without dispersion correction (*5*).

The fact that inclusion of the dispersion time constant, τ, as a fourth fitting parameter did not significantly change the time delays, Δt, calculated by the fitting approach with a fixed value of $\tau = 5$ sec is yet another confirmation of the reliability of the proposed simultaneous correction method. It indicates that the interaction between Δt and τ is minimal, allowing an accurate estimation of the two parameters. The fitted dispersion time constants from our six studies varied between 2.8 and 5.6 sec with a mean of 4.0 sec, very close to the fixed value of $\tau = 5$ sec estimated from cardiac PET studies (*5*). This estimate relates to dispersion between the left ventricle of the heart and the radial artery only and, therefore, is an overestimate. Our fitted values of τ relate to net dispersion, i.e., the dispersion between the heart and the radial artery minus the dispersion between the heart and the brain.

As was to be expected, we found that the longer Δt, the larger the fitted dispersion time constant, τ (Table 5). This observation again points to the obvious link between time delay (transit time difference) and dispersion. The simultaneous correction method described in this paper, therefore, represents a logical step towards a

more adequate and realistic treatment of the two phenomena.

ACKNOWLEDGMENTS

This work was supported by Grant SP-5 from the Medical Research Council of Canada and the Isaac Walton Killam Fellowship Fund of the Montreal Neurological Institute. We thank the technical staff of the McConnell Brain Imaging Centre, the Medical Cyclotron Unit and the Neurophotography Department for their assistance. Special thanks are due to Dr. Hidehiro Iida from the Research Institute for Brain and Blood Vessels, Akita, Japan, as well as to Drs. A. C. Evans, A. Gjedde, A. M. Hakim and Mr. S. Marrett for many helpful discussions. The kind assistance of Dr. R. Zatorre in the analysis of variance is gratefully acknowledged.

REFERENCES

1. Iida H, Higano S, Tomura N, et al. Evaluation of regional differences of tracer appearance time in cerebral tissues using [^{15}O] water and dynamic positron emission tomography. *J Cereb Blood Flow Metab* 1988; 8:285–288.
2. Herscovitch P, Markham J, Raichle ME. Brain blood flow measured with intravenous O-15 H2O. 1. Theory and error analysis. *J Nucl Med* 1983; 24:782–789.
3. Raichle ME, Martin WRW, Herscovitch P, Mintun MA, Markham J. Brain blood flow measured with intravenous O-15 H2O. II. Implementation and validation. *J Nucl Med* 1983; 24:790–798.
4. Dhawan V, Conti J, Mernyk M, Jarden JO, Rottenberg DA. Accuracy of PET rCBF measurements: effect of time shift between blood and brain radioactivity curves. *Phys Med Biol* 1986; 31:507–514.
5. Iida H, Kanno I, Miura S, Murakami M, Takahashi K, Uemura K. Error analysis of a quantitative cerebral blood flow measurement using O-15 H2O autoradiography and positron emission tomography, with respect to the dispersion of the input function. *J Cereb Blood Flow Metab* 1986; 6:536–545.
6. Koeppe RA, Hutchins GD, Rothley JM, Hichwa RD. Examination of assumptions for local cerebral blood flow studies in PET. *J Nucl Med* 1987; 28:1695–1703.
7. Kanno I, Iida H, Miura S, et al. A system for cerebral blood flow measurement using an O-15 H2O autoradiographic method and positron emission tomography. *J Cereb Blood Flow Metab* 1987; 7:143–153.
8. Dhawan V, Jarden O, Strother SC, Rottenberg DA. Error in parameter estimates from 82Rb/PET studies of blood-brain barrier (BBB) permeability: effect of blood curve smearing and the time shift between blood and brain radioactivity curves. *J Cereb Blood Flow Metab* 1987; 7(suppl 1):S444.
9. Meyer E, Tyler JL, Thompson CJ, Redies C, Diksic M, Hakim AM. Estimation of cerebral oxygen utilization rate by single bolus oxygen-15 O2 inhalation and dynamic positron emission tomography. *J Cereb Blood Flow Metab* 1987a; 7:403–414.
10. Thompson CJ, Dagher A, Meyer E, Evans AC. Imaging performance of a dynamic positron emission tomograph: Positome IIIp. *IEEE Trans Med Imag* 1986; 5:183–198.
11. Cooke BE, Evans AC, Fanthome EA, Alarie R, Sendyk AM. Performance figures and images from the Therascan 3128 positron emission tomograph. *IEEE Trans Nucl Sci* NS-31:640–644.
12. Bergström M, Litton J, Eriksson L, Bohm C, Blomqvist G. Determination of object contour from projections for attenuation correction in cranial positron emission tomography. *J Comput Assist Tomogr* 1982; 6:365–372.
13. Madsen MT. A simplified formulation of the gamma variate function [Abstract]. *J Nucl Med* 1987; 28:680.
14. Bevington BR. Data reduction and error analysis for the physical sciences. Chap. 1. McGraw-Hill, 1969.
15. Meyer E, Tyler JL, Thompson CJ, Hakim AM. The time dependence of the O-15 bolus model for CMRO2 measurement by PET with respect to dispersion of the input function [Abstract]. *J Nucl Med* 1987; 28:699.
16. Senda M, Nishizawa S, Shibata T, et al. Effect of arterial blood dispersion on the measurement of cerebral blood flow using PET and O-15 water [Abstract]. *J Nucl Med* 1987; 28:656.
17. Evans AC, Diksic M, Yamamoto YL, et al. Effect of vascular activity in the determination of rate constants for the uptake of ^{18}F-labeled 2-fluoro-2-deoxy-D-glucose: error analysis and normal values in older subjects. *J Cereb Blood Flow Metab* 1986; 6:724–738.
18. Zar JH. Biostatistical analysis. 2nd ed. Englewood Cliffs, NJ: Prentice-Hall, 1984.
19. Frackowiak RSJ, Lenzi G-L, Jones T, Heather JD. Quantitative measurement of regional cerebral blood flow and oxygen metabolism in man using O-15 and positron emission tomography. Theory, procedure, and normal values. *J Comput Assist Tomogr* 1980; 4:727–736.
20. Stokely E. Regional multiparameter estimation from tomographic diffusible tracer clearance curves: modification of the double integral method. *J Cereb Blood Flow Metab* 1985; 5:133–141.
21. Sullivan HG, Allison JD, Kingsbury IV TB, Goode JJ. Analysis of inhalation rCBF data. *Stroke* 1987; 18:495–502.